Langmuir
Article
pubs.acs.org/Langmuir

Fluorescent pH-Sensing Organic/Inorganic Hybrid Mesoporous Silica Nanoparticles with Tunable Redox-Responsive Release Capability

Xuejuan Wan, Di Wang, and Shiyong Liu*

CAS Key Laboratory of Soft Matter Chemistry, Department of Polymer Science and Engineering, Hefei National Laboratory for Physical Sciences at the Microscale, University of Science and Technology of China, Hefei, Anhui 230026, China

Received May 26, 2010. Revised Manuscript Received August 4, 2010

We report on the fabrication of fluorescent pH-sensing organic/inorganic hybrid mesoporous silica nanoparticles (MSN) capable of tunable redox-responsive release of embedded guest molecules. The reversible addition−fragmentation chain transfer (RAFT) copolymerization of *N*-(acryloxy)succinimide (NAS), oligo(ethylene glycol) monomethyl ether methacrylate (OEGMA), and 1,8-naphthalimide-based pH-sensing monomer (NaphMA) at the surface of MSN led to fluorescent organic/inorganic hybrid MSN. The obtained hybrid MSN exhibits excellent water dispersibility and acts as sensitive fluorescent pH probes in the range pH 4−8 due to the presence of NaphMA moieties. After loading with rhodamine B (RhB) as a model drug molecule, P(NAS-*co*-OEGMA-*co*- NaphMA) brushes at the surface of hybrid MSN were cross-linked with cystamine to block nanopore entrances for the effective retention of guest molecules. Taking advantage of disulfide-containing cross-linkers, the release rate of RhB can be easily adjusted by adding varying concentrations of dithiothreitol (DTT), which can cleave the disulfide linkage to open blocked nanopores. The increase of DTT concentration from 0 to 20 mM led to 20−30 times enhancement of RhB release rate. The reported multifunctional hybrid MSN augurs well for applications in controlled-release nanocarriers, cell and tissue imaging, and clinical diagnosis.

Introduction

Self-assembled smart drug nanocarriers such as liposomes, block copolymer micelles, vesicles, and capsules that can trap guest molecules and release them under a specific external stimulus (e.g., pH, temperature, light, and bioactive molecules) or a combination of them have been extensively explored in the past decades.[1−4] Generally, these supramolecular assemblies possess inherent limitations such as insufficient structural stability and low drug loading efficiency. After intravenous administration, the high dilution and large shear forces during blood circulation can lead to structural disintegration of drug nanocarriers. For block copolymer micelles and vesicles, core or shell cross-linking approaches have been utilized to partially solve the structural stability problem.[5] However, their use as controlled delivery vehicles for hydrophilic drugs still poses a considerable challenge.

As an alternative to drug nanocarriers constructed from polymeric materials, inorganic materials such as mesoporous silica nanoparticles (MSN) hold great promise as new-generation smart drug nanocontainers due to their high stability, large surface areas, tunable pore sizes, and abundant surface functionalization sites.[6−10] One of the key issues in designing MSN-based drug delivery vehicles is to develop novel strategies for the on/off switching of nanopores, i.e., blocking the nanopore entrances after encapsulating drug molecules and uncapping them for triggered release under specific external stimuli. Previously, various types of nanoparticles,[11−16] organic molecules,[17−26] and polymer chains or brushes[27−30] with hydrodynamic sizes comparable to or larger than the nanopore entrances of MSN were

*To whom correspondence should be addressed. E-mail: sliu@ustc.edu.cn.

(1) Peer, D.; Karp, J. M.; Hong, S.; FarokHzad, O. C.; Margalit, R.; Langer, R. *Nat. Nanotechnol.* **2007**, *2*, 751–760.
(2) Torchilin, V. P. *Adv. Drug Delivery Rev.* **2006**, *58*, 1532–1555.
(3) Discher, D. E.; Ortiz, V.; Srinivas, G.; Klein, M. L.; Kim, Y.; David, C. A.; Cai, S. S.; Photos, P.; Ahmed, F. *Prog. Polym. Sci.* **2007**, *32*, 838–857.
(4) Rapoport, N. *Prog. Polym. Sci.* **2007**, *32*, 962–990.
(5) Thurmond, K. B.; Kowalewski, T.; Wooley, K. L. *J. Am. Chem. Soc.* **1996**, *118*, 7239–7240.
(6) Stein, A.; Melde, B. J.; Schroden, R. C. *Adv. Mater.* **2000**, *12*, 1403–1419.
(7) Saha, S.; Leung, K. C. F.; Nguyen, T. D.; Stoddart, J. F.; Zink, J. I. *Adv. Funct. Mater.* **2007**, *17*, 685–693.
(8) Vallet-Regi, M.; Balas, F.; Arcos, D. *Angew. Chem., Int. Ed.* **2007**, *46*, 7548–7558.
(9) Manzano, M.; Vallet-Regí, M. *J. Mater. Chem.*, DOI: 10.1039/b922651f.
(10) Wang, Y. J.; Caruso, F. *Chem. Mater.* **2005**, *17*, 953–961.
(11) Giri, S.; Trewyn, B. G.; Stellmaker, M. P.; Lin, V. S. Y. *Angew. Chem., Int. Ed.* **2005**, *44*, 5038–5044.
(12) Vivero-Escoto, J. L.; Slowing, I. I.; Wu, C. W.; Lin, V. S. Y. *J. Am. Chem. Soc.* **2009**, *131*, 3462–3463.
(13) Torney, F.; Trewyn, B. G.; Lin, V. S. Y.; Wang, K. *Nat. Nanotechnol.* **2007**, *2*, 295–300.
(14) Lee, J. E.; Lee, N.; Kim, H.; Kim, J.; Choi, S. H.; Kim, J. H.; Kim, T.; Song, I. C.; Park, S. P.; Moon, K. M.; Hyeon, T. *J. Am. Chem. Soc.* **2010**, *132*, 552–557.
(15) Liu, R.; Zhang, Y.; Zhao, X.; Agarwal, A.; Muller, L. J.; Feng, P. Y. *J. Am. Chem. Soc.* **2010**, *132*, 1500–1501.
(16) Aznar, E.; Marcos, M. D.; Martinez-Manez, R.; Sancenon, F.; Soto, J.; Amoros, P.; Guillem, C. *J. Am. Chem. Soc.* **2009**, *131*, 6833–6843.
(17) Nguyen, T. D.; Leung, K. C. F.; Liong, M.; Liu, Y.; Stoddart, J. F.; Zink, J. I. *Adv. Funct. Mater.* **2007**, *17*, 2101–2110.
(18) Schlossbauer, A.; Kecht, J.; Bein, T. *Angew. Chem., Int. Ed.* **2009**, *48*, 3092–3095.
(19) Patel, K.; Angelos, S.; Dichtel, W. R.; Coskun, A.; Yang, Y. W.; Zink, J. I.; Stoddart, J. F. *J. Am. Chem. Soc.* **2008**, *130*, 2382–2383.
(20) Mal, N. K.; Fujiwara, M.; Tanaka, Y. *Nature* **2003**, *421*, 350–353.
(21) Lu, J.; Choi, E.; Tamanoi, F.; Zink, J. I. *Small* **2008**, *4*, 421–426.
(22) Angelos, S.; Yang, Y. W.; Patel, K.; Stoddart, J. F.; Zink, J. I. *Angew. Chem., Int. Ed.* **2008**, *47*, 2222–2226.
(23) Climent, E.; Bernardos, A.; Martinez-Manez, R.; Maquieira, A.; Marcos, M. D.; Pastor-Navarro, N.; Puchades, R.; Sancenon, F.; Soto, J.; Amoros, P. *J. Am. Chem. Soc.* **2009**, *131*, 14075–14080.
(24) Park, C.; Kim, H.; Kim, S.; Kim, C. *J. Am. Chem. Soc.* **2009**, *131*, 16614–16615.
(25) Ferris, D. P.; Zhao, Y. L.; Khashab, N. M.; Khatib, H. A.; Stoddart, J. F.; Zink, J. I. *J. Am. Chem. Soc.* **2009**, *131*, 1686–1687.
(26) Bernardos, A.; Aznar, E.; Marcos, M. D.; Martinez-Manez, R.; Sancenon, F.; Soto, J.; Barat, J. M.; Amoros, P. *Angew. Chem., Int. Ed.* **2009**, *48*, 5884–5887.
(27) Liu, R.; Zhao, X.; Wu, T.; Feng, P. Y. *J. Am. Chem. Soc.* **2008**, *130*, 14418–14419.
(28) Liu, R.; Zhang, Y.; Feng, P. Y. *J. Am. Chem. Soc.* **2009**, *131*, 15128–15129.

Scheme 1. Schematic Illustration for the Synthesis of pH-Sensing Organic/Inorganic Hybrid Mesoporous Silica Nanoparticles (MSN) Coated with P(NAS-*co*-OEGMA-*co*-NaphMA) Brushes, Their Cross-Linking with Cystamine, and Redox-Responsive Release of Embedded Rhodamine B (RhB) Dyes

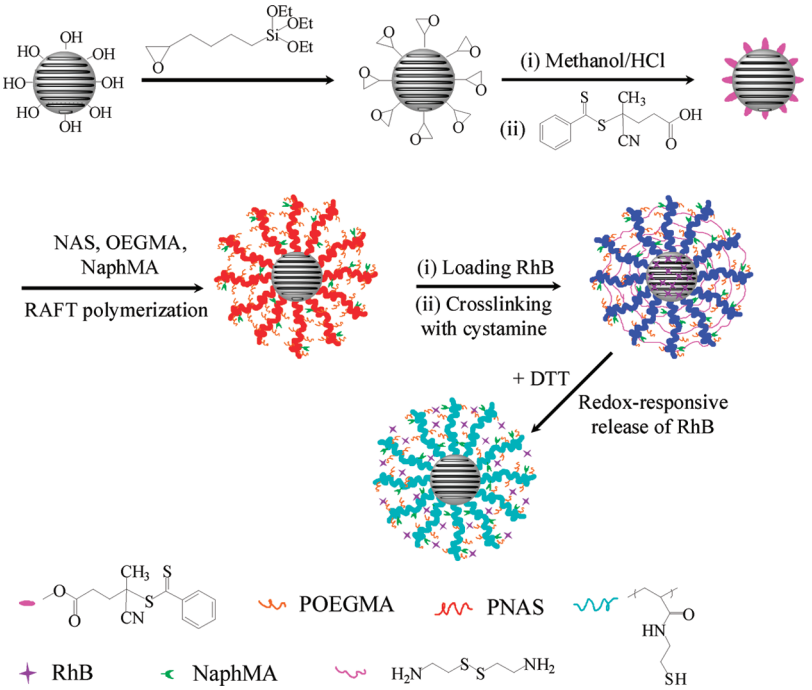

employed to effectively prevent the release of encapsulated guest molecules. As for the triggered release mechanisms, photoswitchable cis−trans isomerization,[21,25] photolabile[12,16,17,24] or pH-labile[15,16] covalent linkages, enzyme-catalyzed degradation,[19,24] and reversible noncovalent interactions (electrostatic interaction,[12] supramolecular recognition[16,22,23,25]) have been typically employed.

Recently, Lin et al.[12] utilized positively charged gold nanoparticles to block the nanopores of MSN via electrostatic interaction. Upon UV irradiation, gold nanoparticles exhibit surface charge reversal behavior due to the presence of photolabile *o*-nitrobenzyl ester moiety, leading to the uncapping of MSN nanopores. Zink and Stoddart et al.[25] functionalized the MSN surface with azobenzene derivatives, and their supramolecular recognition with β-cyclodextrin (β-CD) can effectively block the MSN nanopores. To avoid the uncontrolled release of guest molecules from polymer brush-coated MSN, Feng et al.[27] synthesized poly(*N*-(acryloxy)succinimide) (PNAS)-coated MSN via surface-initiated reversible addition−fragmentation chain transfer (RAFT) polymerization and cross-linked the polymer brushes with cystamine to cap the MSN nanopore entrances. The uncapping can be easily achieved via the addition of dithiothreitol (DTT) to induce cleavage of disulfide bonds. Most recently, they further modified PNAS-coated MSN with β-CD through a disulfide linkage, the addition of diazo linker can also cross-link the polymer brushes; most importantly, the uncapping can be induced by multiple stimuli, such as photoirradiation, the addition of DTT, or excess β-CD.[28] It should be noted that all the above examples of MSN-based drug nanocarriers have focused on developing new triggered-release strategies. Under certain circumstances, it is highly desirable to endow MSN-based nanocarriers with multifunctions such as detection and targeted delivery.

For example, in living organisms, intracellular pH plays key roles in enzyme, cell, and tissue activities, and microenvironments in endosomes (pH 5.5−6) and lysosomes (pH 4.5−5) are mildly acidic. Besides, some tumor cells possess lower extracellular pH (pH 6.4−6.9) compared to normal tissues (pH 7.2−7.4). Thus, monitoring pH changes and gradients are quite important to determine the efficiency of pharmaceutical therapy, diagnose certain cancer diseases, and investigate cellular internalization pathways. If MSN-based drug nanocarriers are endowed with pH-sensing ability, they might be quite useful in practical applications for simultaneous chemotherapy and the monitoring of therapeutic efficiency; moreover, this novel type of multifunctional MSN-based nanocarriers can be quite advantageous to investigate the drug nanocarriers−cell interactions and understand the underlying mechanism.

Herein, we report on the fabrication of multifunctional fluorescent organic/inorganic hybrid MSN possessing pH-probing and tunable redox-responsive release properties. Random copolymers composed of *N*-(acryloxy)succinimide (NAS), oligo(ethylene glycol) monomethyl ether methacrylate (OEGMA), and 1,8-naphthalimide-based fluorescent pH-sensing monomer (NaphMA) were anchored at the surface of MSN via surface-initiated RAFT polymerization (Scheme 1). The obtained hybrid MSN exhibits excellent water dispersibility and can act as sensitive fluorescent pH probe in the range of pH 4−8 due to the presence of NaphMA moieties. Moreover, after loading with model drug molecules, rhodamine B (RhB), and cross-linking the polymer brushes with cystamine, the redox-responsive release of encapsulated guest molecules from organic/inorganic MSN can be facilely tuned by varying the concentrations of externally added DTT. As far as we know, this represents the first report of endowing MSN-based triggered-release nanocarriers with pH sensing functions.

Results and Discussion

Synthetic schemes employed for the preparation of multifunctional fluorescent organic/inorganic hybrid MSN possessing pH-probing ability and tunable redox-responsive release properties

(29) Hong, C. Y.; Li, X.; Pan, C. Y. *J. Phys. Chem. C* **2008**, *112*, 15320–15324.
(30) Pollak, A.; Blumenfeld, H.; Wax, M.; Baughn, R. L.; Whitesides, G. M. *J. Am. Chem. Soc.* **1980**, *102*, 6324–6336.

Scheme 2. Synthetic Schemes Employed for the Preparation of 1,8-Naphthalimide-Based pH-Sensing Fluorescent Monomer (NaphMA, 4)

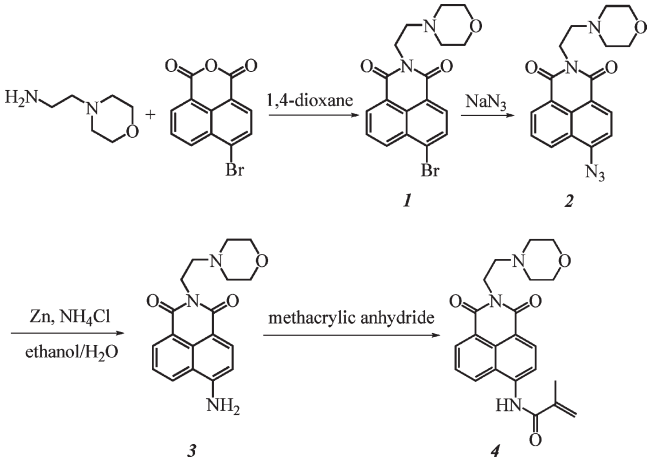

are shown in Scheme 1. Surface-initiated RAFT copolymerization of NAS, OEGMA, and 1,8-naphthalimide-based fluorescent pH-sensing monomer (NaphMA) from MSN led to organic/inorganic hybrid MSN coated with P(NAS-*co*-OEGMA-*co*- NaphMA) random copolymer brushes. They were subject to the loading of model drug molecules, RhB, and subsequent cross-linking with cystamine.

Synthesis of 1,8-Naphthalimide-Based pH-Sensing Monomer (NaphMA, 4). pH-sensing fluorescent monomer, NaphMA (**4**), was synthesized via four steps, starting from 4-bromo-1,8-naphthalic anhydride (Scheme 2). The reaction between 4-bromo-1,8-naphthalic anhydride and 4-(2-aminoethyl)morpholine was performed in 1,4-dioxide under reflux. The ^{1}H NMR spectrum of compound **1** is shown in Figure S1 (Supporting Information). Resonance signals at 3.49 ppm (peak a) and 2.42 ppm (peak b) are assigned to methylene protons in the morpholine moiety. All other resonance signals can be well assigned, indicating the successful preparation of compound **1**. Compound **2** was synthesized by the substitution reaction of compound **1** in the presence of sodium azide. Its ^{1}H NMR spectrum is shown in Figure S1 (Supporting Information), together with the peak assignments. The resonance signal ascribed to the naphthalimide proton neighboring the bromine substituent (peak f) shifts from 7.9 to 7.4 ppm after azidation, accompanied by a considerable shift of other resonance signals of naphthalimide protons in the NMR spectrum of **2**, as compared to those of **1**.

The azide moiety in **2** was converted to amine in the presence of zinc powder and ammonium chloride, and the obtained **3** was further reacted with methacrylic anhydride to give the target compound (**4**). ^{1}H NMR spectra of **3** and **4** are shown in Figure S2 (Supporting Information), together with the peak assignments. Compared to those in **2**, resonance signals characteristic of naphthalimide proton (peak f) in the NMR spectrum of **3** exhibit considerable shift from 7.4 ppm to 6.8 ppm, indicating that azido moieties were completely converted to amine functionality. After the amidation reaction, we can clearly observe the appearance of methacrylamide double bond at $\delta = 5.7$ and 6.0 ppm. For all the ^{1}H NMR spectra of compounds **1**−**4**, both peak assignments and peak integral ratios confirm the successful preparation of them.

Preparation of Hybrid MSN Coated with P(NAS-*co*-OEGMA-*co*-NaphMA) Brushes. First, MCM-41 was prepared according to literature process,[32,33] which has been well-known to produce spherical mesoporous silica nanoparticles with relatively narrow size and homogeneous pore distribution. The obtained MCM-41 was treated with EHTES to introduce epoxy functionalities, followed by removing CTAB templates by refluxing overnight in a methanolic solution of HCl (1.5 M). During the same process, epoxy moieties at the surface of MSN were also converted to 5,6-dihydroxyhexyl functionalities. The ordered mesoporous structure and the particle morphology are confirmed by X-ray diffraction (XRD, Figure S3, Supporting Information), HRTEM (Figure 1), and N_2 adsorption measurements (Figure S4, Supporting Information). The obtained MSN possesses an average diameter of 150 ± 15 nm (Figure 1a,b) with BET surfaces of approximately 1024 m^2/g and an average pore size of ~2.6 nm (Figure S4, Supporting Information).

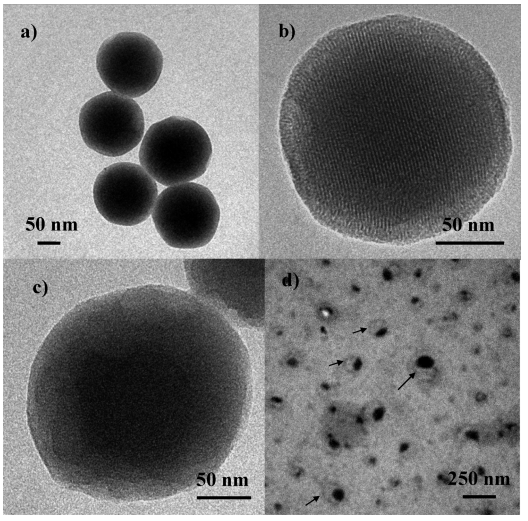

Figure 1. TEM images of (a) and (b) mesoporous silica MCM-41, (c) organic/inorganic hybrid MSN coated with P(NAS-*co*-OEGMA-*co*-NaphMA) brushes, and (d) organic/inorganic hybrid MSN coated with cross-linked polymer brushes subjected to HF treatment for 15 min.

Further functionalization of MSN with RAFT agents was achieved via DCC-mediated esterification in the presence of a RAFT agent, CPAD. Decreasing weight retentions from 96.7% for naked MSN, 95.4% for epoxy-functionalized MSN, and 93.3% for CPAD-functionalized MSN are observed in the TGA curves (Figure 2). Besides, a new band at 1730 cm^{-1} characteristic of the ester carbonyl group appears for CPAD-functionalized MSN in the FT-IR spectrum (Figure S5, Supporting Information), clearly indicating the covalent attachment of CPAD agent onto MSN. However, it is quite difficult to calculate the density of functionalization sites at the surface of MSN because the volumetric mass density of MSN cannot be accurately determined.

Three comonomers were chosen for the surface-initiated RAFT copolymerization from MSN. Hydrophilic OEGMA was incorporated into grafted polymer brushes to enhance the water dispersibility of hybrid MSN with improved biocompatibility, whereas the incorporation of NaphMA residues can endow organic/inorganic hybrid MSN with pH-sensing ability. NAS residues are well-known for their remarkable reactivity for primary amines. Thus, the incorporation of NAS into polymer brushes can allow for the facile cross-linking with cystamine. Previously, McCormick et al.[31,34] reported the synthesis of

(31) Mitsukami, Y.; Donovan, M. S.; Lowe, A. B.; McCormick, C. L. *Macromolecules* **2001**, *34*, 2248–2256.
(32) Radu, D. R.; Lai, C. Y.; Wiench, J. W.; Pruski, M.; Lin, V. S. Y. *J. Am. Chem. Soc.* **2004**, *126*, 1640–1641.
(33) von Werne, T.; Patten, T. E. *J. Am. Chem. Soc.* **2001**, *123*, 7497–7505.
(34) Li, Y. T.; Lokitz, B. S.; McCormick, C. L. *Macromolecules* **2006**, *39*, 81–89.

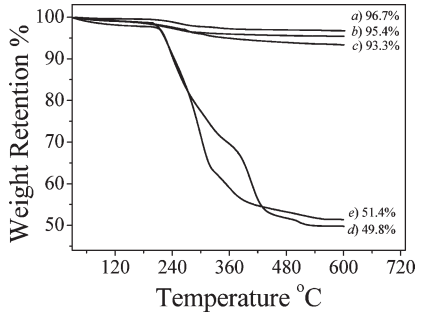

Figure 2. TGA curves of (a) pure mesoporous silica MCM-41, (b) epoxy-functionalized MSN, (c) mesoporous silica surface functionalized with RAFT mediating agent, and organic/inorganic hybrid MSN coated with P(NAS-*co*-OEGMA-*co*-NaphMA) brushes (d) before and (e) after cross-linking with cystamine.

PEO-P(DMA-*co*-NAS)-PNIPAM triblock copolymer in which PEO, DMA, and NIPAM are poly(ethylene oxide), *N*,*N*-dimethylacrylamide, and *N*-isopropylacrylamide, respectively. Taking advantage of the NAS residues, self-assembled micelles at elevated temperatures can be cross-linked with cystamine. Moreover, the cross-linking is reversible due to the presence of redox-reactive disulfide bonds.

The surface-initiated RAFT polymerization of NAS, OEGMA, and pH-sensing monomer NaphMA at the surface of MSN was conducted in 1,4-dioxane at 70 °C with a feed ratio of 6:4:0.08. The obtained hybrid MSN exhibits much better aqueous dispersibility compared to the as-prepared MSN. The aqueous dispersion (0.1 g/L) of hybrid MSN shows no macroscopic phase separation upon standing at room temperature for more than 1 week. HRTEM was employed to characterize the core−shell nanostructures of organic/inorganic hybrid MSN, and the results are shown in Figure 1. The pore channels of the as prepared MSN are homogeneously arranged, endowing adequate space for trapping guest molecules. As for hybrid MSN coated with P(NAS-*co*-OEGMA-*co*-NaphMA) brushes, a polymeric nanoshell can be clearly discerned at the exterior surface of MSN. The thickness of the polymer brushes is approximately 20 nm. After RAFT polymerization, the weight retention of organic/inorganic hybrid MSN further decreases to 49.8%, as evidenced from TGA analysis results (Figure 2). Using CPAD-functionalized MSN as a reference, the weight fraction of P(NAS-*co*-OEGMA-*co*- NaphMA) brush layers in organic/inorganic hybrid MSN is ~46.6%.

FT-IR spectra of pure mesoporous silica MCM-41 and hybrid MSN coated with P(NAS-*co*-OEGMA-*co*-NaphMA) brushes are shown in Figure S5 (Supporting Information). As compared to the case of pure MSN, new bands at 1809, 1780, and 1740 cm^{-1} appeared in hybrid MSN before cross-linking. The former two bands are characteristic of cyclic carbonyl in NAS moieties, whereas absorbance peaks at ~1740 cm^{-1} are characteristic of the ester carbonyl of both OEGMA and NAS residues. Thus, FT-IR analysis results indicate the successful surface grafting. For the characterization of molecular weight and molecular weight distribution of grafted polymer chains, hybrid MSN coated with P(NAS-*co*-OEGMA-*co*-NaphMA) brushes were reacted with *n*-butylamine to fully convert reactive NAS moieties to *N*-*n*-butylacrylamide (*n*BAM) residues, grafted polymer chains were then cleaved from the surface of MSN by treating with hydrofluoric acid.

The GPC trace of cleaved P(*n*BAM-*co*-OEGMA-*co*-NaphMA) chains is shown in Figure S6 (Supporting Information), revealing an M_n of 37 300 and an M_w/M_n of 1.23. The relatively narrow polydispersity index and symmetric GPC elution peak implies that the surface-initiated RAFT polymerization is conducted in a controlled manner. The ^1H NMR spectrum of cleaved polymer chains is also shown in Figure S6 (Supporting Information). The *n*BAM/OEGMA molar ratio is calculated to be 5.8:4.2 on the basis of the integral ratio of peaks a to f. As the NaphMA feed ratio is quite low (~0.8 mol %), its molar content (~0.7 mol %) was determined by fluorescence measurements in methanol.

DTT-Regulated Release of Guest Molecules from Hybrid MSN Coated with Cross-linked Polymer Brushes. Previously, Hong et al.[29,35] synthesized hybrid MSN coated with pH-responsive poly(acrylic acid) (PAA) or thermoresponsive poly(*N*- isopropylacrylamide) (PNIPAM) brushes. Although the release profile of encapsulated drugs can be adjusted via external pH or temperature changes, covalently grafted polymer brushes can not completely block nanopore entrances and drug leakage from MSN-based nanocarriers before arriving at the target site might occur. In recent works by Feng et al.[27] concerning hybrid MSN-based nanocarriers, polymer brushes cross-linked by disulfide-containing difunctional species, or supramolecular recognition between β-CD and azobenzene moieties[28] were employed to effectively block nanopore entrances. Most importantly, triggered release of guest molecules can be achieved. In the current work, we copolymerized water-soluble monomer (OEGMA) and pH-sensing monomer (NaphMA) into PNAS brushes grafted at the surface of hybrid MSN to enhance its water-dispersibility and endow nanocarriers with sensing functions.

P(NAS-*co*-OEGMA-*co*-NaphMA) brushes anchored at the surface of MSN were cross-linked with cystamine. A comparison of TGA analysis results (Figure 2) of hybrid MSN coated with polymer brushes before and after cross-linking, 49.8% and 51.4% weight retention, respectively, reveals that ~90% of NAS residues have reacted with cystamine. Considering that the amidation reaction of NAS with cystamine might also occur in an intrachain manner, which does not contribute to effective cross-linking, the actual degree of cross-linking should be less than 90%. The FT-IR spectrum of organic/inorganic hybrid MSN coated with cross-linked brushes is also shown in Figure S5 (Supporting Information). After cross-linking, absorption bands at around 1780−1810 cm^{-1} characteristic of the cyclic carbonyl group in NAS completely disappear, accompanied by the appearance of absorption peaks at around 1558−1643 cm^{-1}, which are characteristic of amide functionalities. Thus, both TGA and FT-IR results confirm successful cross-linking of P(NAS-*co*-OEGMA-*co*-NaphMA) brushes. XRD results (Figure S3, Supporting Information) indicate that after cross-linking, peak intensities at 110, 200, and 210 considerably decrease, which should be ascribed to the pore-filling effect induced by cross-linking. Nitrogen adsorption−desorption experiments are shown in Figure S4 (Supporting Information). A typical type IV isotherm of mesoporous materials was observed for the as prepared MSN, whereas organic/inorganic hybrid MSN coated with cross-linked polymer brushes apparently exhibits isotherm characteristic of nonporous materials. Moreover, BET surface areas sharply decreased to 86.7 m^2/g for hybrid MSN coated with cross-linked brushes. This indicates that the entrances of MSN nanopores have been effectively capped. To verify the successful cross-linking of P(NAS-*co*-OEGMA-*co*-NaphMA) brushes, the hybrid MSN was further treated with HF for 15 min, and the actual morphology was examined by TEM (Figure 1d). We can clearly observe the presence of nanocapsules (Figure 1d, diffuse coronas around spots with higher contrast). This suggests that the grafted polymer brushes were successfully cross-linked.

(35) Hong, C. Y.; Li, X.; Pan, C. Y. *J. Mater. Chem.* **2009**, *19*, 5155–5160.

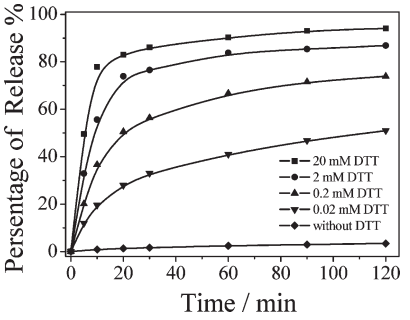

Figure 3. Time evolution of dye release in the presence of varying concentrations of DTT (0−20 mM) for organic/inorganic hybrid MSN coated with cross-linked polymer brushes and encapsulated with RhB.

RhB was then utilized as a model drug to evaluate the controlled release capability of hybrid MSN coated with cross-linked polymer brushes. Release profiles of RhB from hybrid MSN coated with cross-linked polymer brushes were then determined, and the results are shown in Figure 3. In the absence of DTT, the release of RhB is very slow, indicating that the cross-linking reaction can effectively block nanopore outlets. On the other hand, when DTT concentration varies in the range 0−20 mM, we can apparently observe the dramatic enhancement of RhB release rate, which increases with increasing DTT concentrations. DTT can induce the cleavage of disulfide cross-linker, leading to the opening of blocked nanopore entrances. A comparison of release profiles obtained in the presence of 0.02 and 20 mM DTT revealed that low concentrations of DTT are advantageous for steady and controlled RhB release. By changing the DTT concentration in the range of 0−20 mM, we can finely adjust the RhB release profiles. Additionally, the copolymerization of OEGMA residues into polymer brushes can considerably improve the water dispersibility of hybrid MSN.

Organic/Inorganic Hybrid MSN for Fluorescent pH Sensing. The probing of pH gradients and changes are quite crucial to determine the efficiency of pharmaceutical therapy, diagnose certain cancer diseases, and investigate cellular internalization pathways. The choice of suitable fluorescent dyes, or a combination of them, is quite critical for the construction of suitable pH probes. Among them, small molecule naphthalimide derivatives containing arenedicarboximide fluorophores and amine acceptors for protons are quite intriguing.[36,37] The protonation or deprotonation of amine moieties can induce the fluorescence on−off switching of naphthalimide reporters via the photoinduced electron transfer (PET) mechanism, leading to the sensitive probing of pH changes. Naphthalimide-based pH-detecting motifs can even be physically embedded into polymer films to construct optode macro devices, which can be applied in practical circumstances. However, small molecule fluorescent pH probes physically embedded in a polymer matrix have inherent limitations such as leaching and poor water solubility. In the current case, we choose to covalently attach the naphthalimide-based pH-detecting motif to hydrophilic polymer brushes anchored on water-dispersible hybrid MSN via the RAFT copolymerization approach.

1,8-Naphthalimide-based fluorescent pH-sensing monomer (NaphMA, **4**) contains a morpholine acceptor for protons, an arenedicarboximide fluorescence reporter, and a C_2 spacer. In agreement with the spectrofluorometric properties of other naphthalimide-based derivatives as reported by Wolfbeis' research group,[36] the absorbance spectra of **4** exhibit nearly no changes over the pH range 3−10 (Figure S7, Supporting Information). This advantage is quite important for the construction of pH probes with good reliability and repeatability. We then tested the pH-sensing capability of hybrid MSN coated with cross-linked P(NAS-*co*-OEGMA- *co*-NaphMA) chain brushes without loading of guest molecules, and the results are shown in Figure 4. We can clearly observe that decreasing solution pH in the range 10−3 can lead to the off/on switching of fluorescence intensity. Upon protonation, the morpholine moieties cannot act as effective PET donors compared to their unprotonated state, and this results in the fluorescence enhancement of naphthalimide PET acceptor.

A closer examination of Figure 4 reveals that in the range pH 10−3, the fluorescence intensity can be enhanced ~2 times at the maximum emission wavelength of 478 nm. Most importantly, considerable fluorescence intensity changes occur in the range pH

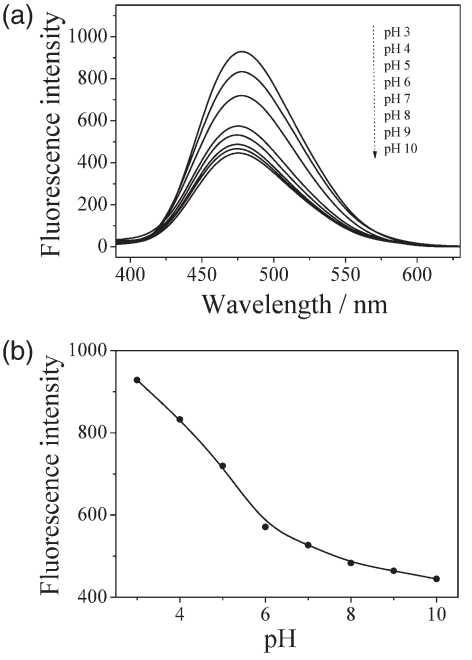

Figure 4. (a) Fluorescence spectra and (b) fluorescence intensity changes (λ_{em} = 478 nm) recorded in the pH range 3−10 (λ_{ex} = 350 nm; slit widths, ex 5 nm and em 5 nm; 25 °C) for organic/inorganic hybrid MSN coated with cross-linked polymer brushes without loading of guest molecules.

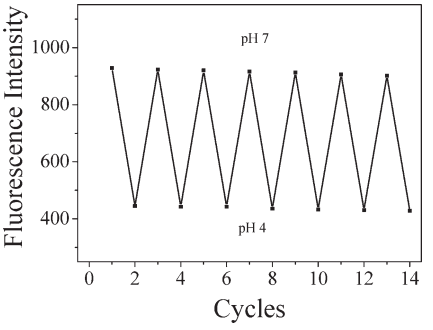

Figure 5. Fluorescence intensity changes recorded for the aqueous dispersion of organic/inorganic hybrid MSN coated with cross-linked polymer brushes under pH cycling of 4−7 upon alternate addition of acid and base.

(36) Daffy, L. M.; de Silva, A. P.; Gunaratne, H. Q. N.; Huber, C.; Lynch, P. L. M.; Werner, T.; Wolfbeis, O. S. *Chem.—Eur. J.* **1998**, *4*, 1810–1815.
(37) de Silva, A. P.; Rice, T. E. *Chem. Commun.* **1999**, 163–164.

5−7, which proves to be a suitable window for monitoring intracellular pH changes and diseased tissues. We also checked the reversibility of pH-induced fluorescence intensity changes. As shown in Figure 5, the fluorescence intensity of the aqueous dispersion of organic/inorganic hybrid MSN coated with cross-linked P(NAS-*co*-OEGMA-*co*-NaphMA) brushes exhibit excellent reversibility upon seven pH cycling between pH 7 and 4. A combination of these results clearly confirms that the synthesized water-dispersible hybrid MSN can act as sensitive and reliable pH probes, which are ideal for in vitro and in vivo pH sensing applications. It should be noted that the current hybrid MSN-based probe design employs fluorescence intensity for pH calibration, which is subjected to limitations such as background interference. Fluorescent ratiometric pH probes based on the fluorescence resonance energy transfer (FRET) mechanism might be more ideal, and further works toward this aspect are currently underway.

Conclusion

We report on the preparation of fluorescent organic/inorganic hybrid mesoporous silica nanoparticles (MSN) with dual capabilities of pH-probing and tunable redox-responsive release of guest molecules. Surface-initiated RAFT polymerization of of *N*-(acryloxy)succinimide (NAS), oligo(ethylene glycol) monomethyl ether methacrylate (OEGMA), and 1,8-naphthalimide-based pH-sensing monomer (NaphMA) from mesoporous silica nanoparticles afforded fluorescent organic/inorganic hybrid MSN coated with cross-linkable polymer brushes, which exhibits good water dispersibility and can act as a sensitive fluorescent pH probe due to the presence of NaphMA moieties. After loading with rhodamine B (RhB) as a model drug molecule, P(NAS-*co*-OEGMA-*co*-NaphMA) brushes at the surface of hybrid MSN were cross-linked with a redox-labile cross-linker, cystamine, to block nanopore entrances. Taking advantage of disulfide-containing cross-linkers, the release rate of RhB can be facilely adjusted by adding varying concentrations of dithiothreitol (DTT). The increase of DTT concentration from 0 to 20 mM led to 20−30 times enhancement of RhB release rate. The reported multifunctional hybrid MSN augurs well for its applications in controlled-release nanocarriers, cell and tissue imaging, and clinical diagnosis.

Acknowledgment. The financial support of the National Natural Scientific Foundation of China (NNSFC) Projects (20874092 and 51033005) and Specialized Research Fund for the Doctoral Program of Higher Education (SRFDP) is gratefully acknowledged.

Supporting Information Available: All the experimental section including synthetic procedures and spectroscopic/analytical data of ^{1}H NMR, GPC, XRD, BET, FT-IR, UV−vis absorption, and spectrofluorometry. This material is available free of charge via the Internet at http://pubs.acs.org.